



HAL
open science

Specific binding of the methyl binding domain protein 2 at the BRCA1-NBR2 locus

Emilie Auriol, Lise-Marie Billard, Frédérique Magdinier, Robert Dante

► To cite this version:

Emilie Auriol, Lise-Marie Billard, Frédérique Magdinier, Robert Dante. Specific binding of the methyl binding domain protein 2 at the BRCA1-NBR2 locus. *Nucleic Acids Research*, 2005, 33 (13), pp.4243-4254. 10.1093/nar/gki729 . hal-01663899

HAL Id: hal-01663899

<https://amu.hal.science/hal-01663899>

Submitted on 14 Dec 2017

HAL is a multi-disciplinary open access archive for the deposit and dissemination of scientific research documents, whether they are published or not. The documents may come from teaching and research institutions in France or abroad, or from public or private research centers.

L'archive ouverte pluridisciplinaire **HAL**, est destinée au dépôt et à la diffusion de documents scientifiques de niveau recherche, publiés ou non, émanant des établissements d'enseignement et de recherche français ou étrangers, des laboratoires publics ou privés.

Specific binding of the methyl binding domain protein 2 at the *BRCA1-NBR2* locus

Emilie Auriol, Lise-Marie Billard, Frédérique Magdinier¹ and Robert Dante*

Laboratoire de Génétique et Cancer, FRE2692 CNRS, UCBL1, 8 avenue Rockefeller, 69373 Lyon cedex 08, France and ¹Laboratory of Molecular Embryology, NIH/NICHD, Bethesda, MD, USA

Received April 15, 2005; Revised and Accepted July 5, 2005

ABSTRACT

The methyl-CpG binding domain (MBD) proteins are key molecules in the interpretation of DNA methylation signals leading to gene silencing. We investigated their binding specificity at the constitutively methylated region of a CpG island containing the bidirectional promoter of the Breast cancer predisposition gene 1, *BRCA1*, and the Near *BRCA1* 2 (*NBR2*) gene. In HeLa cells, quantitative chromatin immunoprecipitation assays indicated that MBD2 is associated with the methylated region, while MeCP2 and MBD1 were not detected at this locus. MBD2 depletion (~90%), mediated by a transgene expressing a small interfering RNA (siRNA), did not induce MeCP2 or MBD1 binding at the methylated area. Furthermore, the lack of MBD2 at the *BRCA1-NBR2* CpG island is associated with an elevated level of *NBR2* transcripts and with a significant reduction of induced-DNA-hypomethylation response. In MBD2 knockdown cells, transient expression of a *Mbd2* cDNA, refractory to siRNA-mediated decay, shifted down the *NBR2* mRNA level to that observed in unmodified HeLa cells. Variations in MBD2 levels did not affect *BRCA1* expression despite its stimulation by DNA hypomethylation. Collectively, our data indicate that MBD2 has specific targets and its presence at these targets is indispensable for gene repression.

INTRODUCTION

In mammals, DNA methylation at CpG islands located within regulatory regions is a crucial event in gene silencing. The various mechanisms leading to methylation-dependent down-regulation of the transcription remain to be fully determined.

However, the discovery of methyl-CpG binding domain (MBD) proteins and their interacting partners provides a direct link between DNA methylation and the establishment of a repressive chromatin architecture (1). The five MBD proteins identified to date share the functional MBD (2). Four of them, MBD1, MBD2, MBD3 and MeCP2, are directly involved in the transcriptional repression of methylated templates in vertebrates and, with the exception of MBD3, bind methylated DNA (3).

MeCP2, the founding member of the MBD family, represses transcription through its interactions with the histone deacetylase–Sin3 complex and the histone 3 lysine 9 trimethyl-transferase Suv39H1 (4–6). MBD3 is part of the histone deacetylase and chromatin remodeling Mi2/NuRD complex, which is targeted to methylated templates in the MeCP1 complex by MBD2 (7,8). In mouse, an interaction between the MBD2 and the Sin3 complex has also been described previously (9). The HDAC complex associated with MBD1 is not yet identified (10), but other MBD1 partners such as histone 3 lysine 9 dimethyl transferase SETDB1 and the chromatin assembly protein 1 have been characterized previously (11,12).

In cell lines, MBD1, MBD2 and MeCP2 transiently repress the expression of genes driven by either strong or weak promoters (13), suggesting some functional redundancies between these proteins. Moreover, both the MBD1 and the MeCP2 proteins are associated, *in vivo*, with the differentially methylated region of the mouse imprinted *U2af1-rs1* gene (14) and, in cancer cell lines, some methylated CpG islands are bound by multiple MBD proteins (15). Since many cell and tissue types express multiple MBD proteins, these data suggest that other members of the family might compensate the absence of a specific MBD. However, functional specificities have been observed. In human, *MeCP2* mutations are the cause of the RETT syndrome (RTT), a neurological disorder associated with motor function impairment that represents one of the most common causes of mental retardation in females (16). In mouse, loss of *Mecp2* leads to phenotypes that

*To whom correspondence should be addressed. Tel: +33 4 78 78 59 22; Fax: +33 4 78 78 27 20; Email: dante@univ-lyon1.fr

Present addresses:

Emilie Auriol and Robert Dante, Unité INSERM 590, Laboratoire d'Oncologie Moléculaire, Centre Léon Bérard, 28 rue Laennec, 69373 Lyon Cedex 08, France
Frédérique Magdinier, Laboratoire de Biologie Moléculaire de la Cellule, CNRS UMR 5161-ENS, Lyon, France

© The Author 2005. Published by Oxford University Press. All rights reserved.

The online version of this article has been published under an open access model. Users are entitled to use, reproduce, disseminate, or display the open access version of this article for non-commercial purposes provided that: the original authorship is properly and fully attributed; the Journal and Oxford University Press are attributed as the original place of publication with the correct citation details given; if an article is subsequently reproduced or disseminated not in its entirety but only in part or as a derivative work this must be clearly indicated. For commercial re-use, please contact journals.permissions@oupjournals.org

resemble some of the symptoms of RTT patients (17,18), indicating a specific function of MeCP2 in the maturation of central nervous system. *Mbd1*^{-/-} mice also show neuronal maturation deficits associated with hippocampal functions (19). Therefore, the involvement of these proteins in different pathways of the central nervous system argues against a functional redundancy between *Mecp2* and *Mbd1*. In addition, mice lacking *Mbd2* do not exhibit specific phenotype except a maternal behavior deficit (20).

Although no global misexpression of endogenous methylated genes has been detected in the first studies, candidate gene approaches have identified some specific target genes. In mouse and rat, *Mecp2* is directly involved in a depolarization-controlled repression of the brain derived neurotrophic factor gene in neurons (21,22), and that of the imprinted *DLX5* gene driven at a distance by *Mecp2* has also been shown previously (23). Specific repression is not restricted to MeCP2. In mouse, loss of *Mbd1* induces small but significant increase in the expression of the endogenous virus, IAP, associated with chromosome instability in cultured neuron cells (19). *Mbd2*^{-/-} mice exhibit a disordered helper T cells differentiation owing to ectopic expression of the *IL4* gene (24).

A comparative study in human cancer cell lines using a chromatin immunoprecipitation (ChIP) assay combined with a CpG island microarray also suggests some specificities, since some cancer-associated hypermethylated genes are bound by multiple MBD proteins while others are associated with a single MBD protein (15). Furthermore, in interphase MCF7 cells, the distribution of MeCP2 does not parallel that of methylated cytosine and heterochromatin, and a selective binding of MeCP2 to some repetitive elements has also been observed previously (25). The mechanisms driving the MBD binding are not yet fully determined. The relative abundance of the MBD proteins might be an important parameter, since it was suggested that there are more methyl-CpGs in the genome than MBD protein molecules (1), and whether MBD1, MBD2 and MeCP2 are randomly associated with sites or segregate owing to other constraints is not yet known.

To address this question, we investigated in HeLa cells, the MBD proteins binding pattern at a CpG island located in the 5' end of the Breast cancer predisposition gene 1 (*BRCA1*). *BRCA1* lies head to head with the Near *BRCA1* 2 gene (*NBR2*) (26). Experiments of site-directed deletions led to the identification of a bidirectional promoter that is embedded within a large CpG island (13). This CpG island contains a region that is constitutively methylated in all human cell lines and tissues, except gametes and preimplantation embryos (27–29). Therefore, this model represents an interesting tool for investigating MBD proteins binding specificity and their effects on transcription at a naturally methylated CpG island.

MATERIALS AND METHODS

Cell culture

Cervix cancer cell line (HeLa) was obtained from ATCC (Rockville, MD) and grown in minimum essential medium (Eagle; Sigma, L'isle d'Abeau, France) supplemented with 10% fetal calf serum. Cells were grown at 37°C in a humidified 5% CO₂ atmosphere.

5-Aza-2'-deoxycytidine treatments

For 5-aza-2'-deoxycytidine (5-aza-dC; Sigma) treatments, cell lines were seeded at low density (3–4 × 10⁵ cells/100 mm dish) 16 h before treatment with a final concentration of 10 μM 5-aza-dC. The medium was changed after 24 h drug addition and every subsequent day. RNAs were isolated after 72 h.

Cell transfections

pCMV-MeCP2-HA (kindly provided by Dr A. Bird), pRev-MBD2 (modified from pCMV-MBD2, kindly provided by Dr A. Bird) and pGL3 basic (Promega, Lyon, France) were transfected using the Exgen500 transfection reagent, according to the manufacturer's instructions (Euromedex, Mundolsheim, France). Cells were collected 48 h after transfection. Transfection efficiency was tested using a CMV-lacZ vector and β-galactosidase activity was observed in >90% of the cells.

Quantification of nucleic acids

Nucleic acids were quantified by densitometry using the Fluorimeter Fluors and the Quantity One software (BioRad, Ivry, France), either from agarose gel containing 1 μg/ml ethidium bromide or dots mixed with an equal volume of a 200-fold diluted solution of RiboGreen (Molecular Probes, Interchim, Montluçon, France).

RNA extraction and quantitative RT-PCR

Total RNA was extracted from cell lines with the RNeasy kit (Qiagen, Courtaboeuf, France) and treated with DNase I using the DNA-free kit (Ambion Inc., Cambridgeshire, UK). After extraction, the integrity of total RNA was examined on a 1.2% agarose gel containing 1 μg/ml ethidium bromide and quantified. cDNA fragment of *NBR2* (from position +146 to +604 from the transcription start site) was amplified by RT-PCR using forward 5'-GAGGTCTCCAGTTTCGGTAA-3' and reverse 5'-GAACCAAGGTGAAGGACCAA-3'. After cloning the PCR product into a pGEM-T easy vector (Promega), a 109 bp long deletion was performed within the *NBR2* cDNA using the restriction endonuclease MaeIII (Roche, Meylan, France). The competitor RNA was synthesized using the Sp6 RNA polymerase according to the manufacturer's instructions (Promega). After DNase I digestion (Ambion Inc.) and RNeasy purification (Qiagen), this competitor RNA was quantified by densitometry and then diluted in the presence of yeast tRNA as a carrier (40 ng/μl; Ambion). For *BRCA1* and *MBD2* quantitative RT-PCR, previously designed competitors were used (30,31).

Equal amounts of total RNA samples (0.6 μg for *NBR2*, 0.3 μg for *BRCA1* and 0.1 μg for *MBD2*) were coamplified with increasing amounts of competitor RNAs in a final volume of 50 μl using the One Step RT-PCR kit, Q solution for *NBR2* (Qiagen) and 0.6 μM of each primers. After a 30 min incubation at 50°C, RT was inactivated by heating at 95°C for 15 min. The PCR amplification was then accomplished in a thermocycler under the following conditions: 35 cycles, 30 s denaturation at 94°C, 1 min annealing at 62°C for *NBR2* and *MBD2*, 64°C for *BRCA1* and 1 min 30 s extension at 72°C. In addition, control experiments for each competitor RNA were performed by omitting the RT to ensure that the signal was the result of RNA and not DNA amplification. PCR products were

analyzed on a 2% agarose gel and quantified. Then, the normalized signals corresponding to the target mRNA and the competitor were plotted against the initial number of competitor molecules added to the test tubes. The abscissa of the intersection of the curves represents an estimation of the equivalence point between the initial amount of the competitor molecules and the number of copies of the mRNA assayed (32).

Protein extraction and western blot analysis

Forty micrograms of whole cell lysates were separated by electrophoresis through SDS–10% polyacrylamide gels and analyzed by western blot (31). For the detection of the MBD proteins, rabbit polyclonal antibodies against MBD2 (kindly provided by Dr P. Wade) or MeCP2 (Upstate Biotechnology, Lake Placid, NY) and mouse monoclonal antibody against MBD1 (Abgent, San Diego, CA), were diluted 1/2000. The secondary anti-rabbit-HRP or anti-mouse-HRP conjugate antibodies were diluted 1/5000. The immunocomplexes were detected using the ECL system (Amersham, Saclay, France).

Quantitative chromatin immunoprecipitation

Cells were washed and scraped off the culture dishes in phosphate-buffered saline, and nuclei were prepared in ice-cold hypotonic buffer (10 mM Tris–HCl, pH 7.4, 10 mM NaCl and 5 mM MgCl₂). Each step was performed on ice and in the presence of a mixture of protease inhibitors (Complete[®]; Roche). After centrifugation, cells were lysed in the hypotonic buffer containing 0.1% NP-40. Nuclei were harvested by centrifugation at 2000 r.p.m. (700 g) and were washed in the same buffer. Nuclear proteins were then cross-linked to DNA by an incubation with 1% formaldehyde for 10 min at room temperature and then for 40 min at +4°C. Cross-linking was stopped by adding 125 mM glycine for 5 min. After centrifugation, the pellets were washed in the hypotonic buffer and resuspended in 1–2 ml of SDS lysis buffer (1% SDS, 10 mM EDTA and 50 mM Tris–HCl, pH 8). Nucleo-protein complexes were sonicated to reduce the length of DNA fragments to 300–600 bp. Insoluble material was removed and the supernatant was collected. Thirty microliters of this fraction was preserved as an input control and the rest was diluted 1:10 in ChIP dilution buffer (ChIP assay Kit; Upstate Biotechnology). The chromatin solution was precleared for 1 h by incubation with 80 µl of salmon sperm DNA–protein A–agarose beads (Upstate Biotechnology). The soluble fraction was collected and 15 µl of monoclonal anti-MBD1 (Abgent), polyclonal anti-MBD1 (Abcam, Cambridge, UK), anti-MBD2 (kindly provided by Dr P. Wade), anti-MeCP2 (Upstate) and anti-mouse IgG (Dakocytomation, Trappes, France) antibodies were added and incubated overnight. Then, for ChIP monoclonal antibodies, 1 µg of rabbit polyclonal anti-mouse antibody (Dakocytomation) was added and incubated for 1 h. After immunoprecipitation, immune complexes were collected by adding 60 µl of salmon sperm DNA–protein A–agarose beads for 1 h. The supernatant corresponding to the unbound fraction was collected. After washing (according to the manufacturer's instructions), complexes were eluted from the beads in 1% SDS and 0.1 M NaHCO₃. This fraction corresponds to the bound (anti-MBD) or the

non-MBD-specific antibodies (anti-mouse IgG) fractions. Cross-links were reversed by heating samples at 65°C in 200 mM NaCl. DNA was recovered by proteinase K digestion, phenol extraction and ethanol precipitation. Finally, DNA samples from the input, unbound, non-MBD-specific antibody and bound fractions were quantified.

Quantitative PCR amplification was performed using a competitor DNA. DNA fragment of the *BRCA1-NBR2* CpG island (from position –1244 to –1004 from the *BRCA1* transcription start site, fragment A) was amplified by PCR using forward 5'-GCTTTTCGCCCACTCGGTCC-3' and reverse 5'-CAGAGCTGGCAGCGGACGGT-3'. After cloning the PCR product into a pGEM-T easy vector (Promega), a single cut within the island fragment was performed using AccIII and an insertion of a 43 bp chemically synthesized duplex-oligonucleotide was accomplished using T4 DNA ligase (Roche). After cloning and purification (Plasmid Maxi Kit; Qiagen), this competitor vector was quantified. Equal amounts (2 ng) of total DNA samples from the input, unbound and bound fractions were coamplified with increasing amounts of competitor plasmid in a final volume of 100 µl using the HotStar *Taq* polymerase kit (Qiagen) and 0.4 µM of each primer. The PCR amplification was accomplished after activation of the *Taq* polymerase (15 min at 95°C and 35 cycles in a thermocycler under the following conditions: 30 s denaturation at 94°C, 1 min annealing at 63°C and 1 min 30 s extension at 72°C). PCR products were analyzed on a 2% agarose gel containing 1 µg/ml ethidium bromide and were quantified by densitometry as described. Then, the normalized signals corresponding to the *BRCA1* CpG island fragment and the competitor were plotted against the initial quantity of competitor molecules added to the test tubes. The abscissa of the intersection of the curves represents an estimation of the equivalence point between the initial amount of the competitor and the quantity of the *BRCA1-NBR2* CpG island fragment in each sample (Supplementary Figure 8s).

We also analyzed three other regions of the methylated *BRCA1-NBR2* CpG island (B, C and D fragments) by performing a semi-quantitative PCR. We amplified equal amounts of total DNA samples (0.5 ng) from the input, unbound and bound fractions, using forward 5'-AAGGGCTCCTC-CAGCACGGC-3' and reverse 5'-TTCTGAGGGACCGA-GTGGGC-3' for the B fragment (from positions –1364 to –1218 from the *BRCA1* transcription start site); forward 5'-TTCAAGCGGGTGCAGGCGG-3' and reverse 5'-CCC-TCTCTGGGCTGGCCGAA-3' for the C fragment (from positions –1389 to –1637); forward 5'-CTGGTGCATA-TAAAATCCTCAGGC-3' and reverse 5'-GCACAGGG-CAAGGCTCAGGA-3' for the D fragment (from positions –1653 to –1928).

As a control, we amplified an unmethylated region including the promoter and the exon 1 of the *BRCA1* gene ('promoter fragment' from position –56 bp to +263 bp) using forward 5'-TAGCCCTTGGGTTCCGTG-3' and reverse 5'-TCACAA-CGCCTTACGCCTC-3'.

PCR was accomplished in a final volume of 100 µl using the HotStar *Taq* polymerase kit (Qiagen) and 0.4 µM of each primer, as described previously, under the following conditions: 30 s denaturation at 94°C, 1 min annealing at 64°C for the fragment B, 66°C for the fragments C and D or at 60°C for the *BRCA1* promoter, and 1 min 30 s extension at 72°C.

PCR products were analyzed and quantified by densitometry. Then, the signals corresponding to the *BRCA1-NBR2* CpG island fragment in the input, unbound and bound fractions were compared.

Stable knockdown of *MBD2* by short interfering RNA and transient reversion

HeLa cells stably expressing small interfering RNA (siRNA) were established as described previously (33). Briefly, the pSUPER_{MBD2} plasmid was generated by cloning the 19 nt sequence 5'-GGAGGAAGTGATCCGAAAA-3' (beginning 575 nt from the translation start site in the mouse *MBD2* mRNA), separated by a spacer from its reverse complement as a BglII/HindIII fragment (synthesized at Prologo, Paris, France) into the pSUPER vector. This vector directs synthesis of RNA from the polymerase III-H1-RNA promoter that is processed in the cell to siRNA. One microgram of pSUPER_{MBD2} was cotransfected with 0.1 µg of a plasmid encoding a geneticin resistance gene into HeLa cells by using Lipofectamine 2000 (Invitrogen, Cergy Pontoise, France). Cells were selected using 1 µg/ml G418 (Roche) for 15 days. Clones were picked and expanded for an additional 20 days and were analyzed for *MBD2* mRNA and protein levels as described previously.

Transient reversion of RNA interference (RNAi) was performed by transfecting HeLa clones with a pRev-*MBD2* vector in which *Mbd2* cDNA sequence was modified at the siRNA-target site. Despite five point mutations (5'-GGAAGA GGTCATTCGCAAA-3', mutated nucleotides are underlined) and also according to the genetic code, the new cDNA sequence encodes a functional Mbd2 protein. This vector was generated by digesting the pCMV-*MBD2* vector (kindly provided by Dr A. Bird) within the *Mbd2* cDNA sequence with KspI (Roche) and AccIII (Promega) endonucleases. This KspI/AccIII fragment was gel-purified (MinElute gel purification Kit; Qiagen) and digested by ApaI and AccI (Roche). A 117 bp double-stranded oligonucleotide (Eurogentec, Seraing, Belgium), containing the five silent point mutations, was introduced into ApaI/AccI site to replace the initial 117 bp fragment. After cloning and sequencing (Biofidal, Vaulx-en-Velin, France), plasmids exhibiting the expected sequence were selected. The transcription of the mutated form of *Mbd2* cDNA allows this mRNA to bypass siRNA-mediated decay. HeLa and *MBD2* knockdown clones were transfected with the resulting vector. Finally, *MBD2* protein expression was assessed after cellular proteins extraction and western blotting.

Sodium bisulfite modification

The sodium bisulfite modification method, followed by the endonuclease restriction of PCR products, was used to determine the CpG methylation pattern. Sodium bisulfite converts unmethylated cytosines to uracils whereas the methylated cytosines remain unmodified. In the resultant modified DNA, uracils are replicated as thymines during PCR amplification (34).

DNA was extracted from cell lines with the QiaAmp DNA Mini Kit (Qiagen). After extraction, the integrity of total DNA was examined on a 1.2% agarose gel and quantified by densitometry. The sodium bisulfite reaction was carried

out as described previously (28). DNA was amplified using strand-specific primers designed to amplify a 304 bp region (methylated region, -1246 to -942 bp from the *BRCA1* transcription start site) and a 250 bp region (unmethylated region, -592 to -343 bp from the *BRCA1* transcription start site) in the CpG island of the *BRCA1* gene. The first round of PCR amplification was accomplished in 100 µl using the HotStar *Taq* DNA polymerase Kit (Qiagen) and 0.4 µM of the primers (methylated region: forward 5'-TTT-TGTTTTGTGTAGGGCGGTT-3' and reverse 5'-CCTTAA-CGTCCATTCTAACCGT-3'; unmethylated region: forward 5'-GTTTATAATTGTTGATAAGTATAAG-3' and reverse 5'-CCCCTCTTTCCGCCCTAAT-3') after 15 min at 95°C for *Taq* polymerase activation and 35 cycles (30 s denaturation at 94°C, 1 min annealing at 55°C for the methylated region or at 56°C for the unmethylated region, and 1 min 30 s extension at 72°C). An aliquot of the first amplification of the methylated region was reamplified with internal primers (forward 5'-TGAGAATTTAAGTGGGGTGT-3' and reverse 5'-AACCCTTCAACCCACCACTAC-3') with the same conditions. PCR products were then analyzed by digestion with the restriction enzymes, CfoI (Roche) and HphI (NEN Biolabs, Saint Quentin Yvelines, France). Digestion products were analyzed on a 2% agarose gel containing 1 µg/ml ethidium bromide.

RESULTS

MBD2 binds to the methylated region of a CpG island flanking the bidirectional *BRCA1-NBR2* promoter

A large CpG island, 2.8 kb in length, lying from nt -1810 to +974 from the *BRCA1* transcription start site (Figure 1) exhibits several features, suggesting that it might be a target for MBD proteins. Indeed, this CpG island is unmethylated in gametes, but regionally methylated (position -2000 to ~-1000) in all tissues and cell lines so far analyzed (27-29), and nuclease protection assays indicate that this methylated region is embedded in a condensed chromatin structure in breast cell lines (29) and in HeLa cells (data not shown).

Quantitative ChIP assays were performed using antibodies directed against MBD1, MBD2 and MeCP2. The analyzed region (nt -1244 to -1004; Figure 1, 'A' segment) is located close to, but does not overlap with, the repetitive element LTR12c (nt -3125 to -1276), which is part of the CpG island (Figure 1). Data obtained from at least three independent ChIP assays for each antibody are shown in Figure 2A. The fractions immunoprecipitated with a non-MBD protein specific antibody (anti-mouse IgG) did not contain enough DNA for PCR assay, indicating an efficient pre-clearing step.

When antibodies against MBD2 are used, the amount of *BRCA1-NBR2* CpG island per ng of total DNA in immunoprecipitated fraction (Figure 2A, 'bound') is higher (~5-fold) than in input or non-retained fractions (Figure 2A, 'input' and 'unbound'). Therefore, these data indicate that the *BRCA1-NBR2* CpG island is specifically immunoprecipitated by the anti-MBD2 antibodies. In contrast, when antibodies against MeCP2 or MBD1 are used, the immunoprecipitated fraction is depleted in *BRCA1-NBR2* CpG island, since the

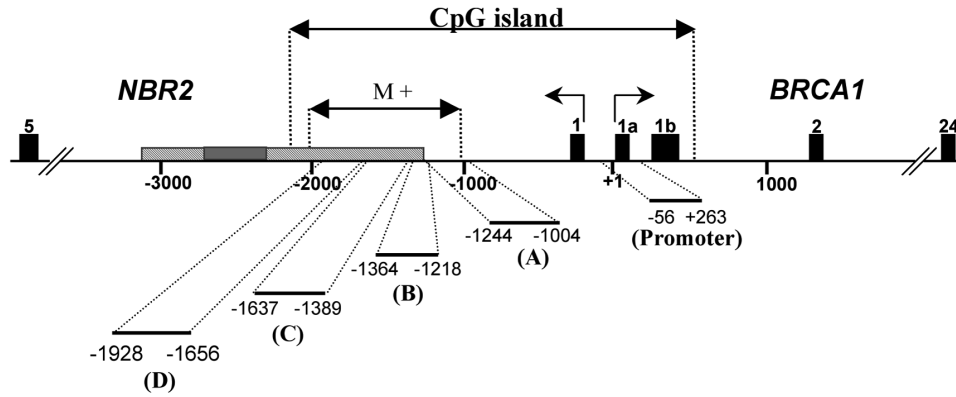


Figure 1. The *BRCA1-NBR2* locus. The *BRCA1* gene is located head to head with the *NBR2* gene and the two genes are separated by a bidirectional promoter (25). Transcription start sites of both genes are arrowed in black. Black box, *BRCA1* and *NBR2* exons. The locus includes a CpG island of 2784 bp in length (%G+C, 57; ObsCpG/ExpCpG, 0.65; CpGProD software, <http://pbil.univ-lyon1.fr>). M+, constitutively methylated region of the CpG island (28); light gray box, LTR12c retroelement; dark gray box, AluY sequence (Repeat Masker software, version 2002). Black lines represent the positions of the fragments amplified by A, competitive PCR; B, C, D and 'promoter', semi-quantitative PCR, after ChIP. Positions are indicated from the *BRCA1* transcription start site.

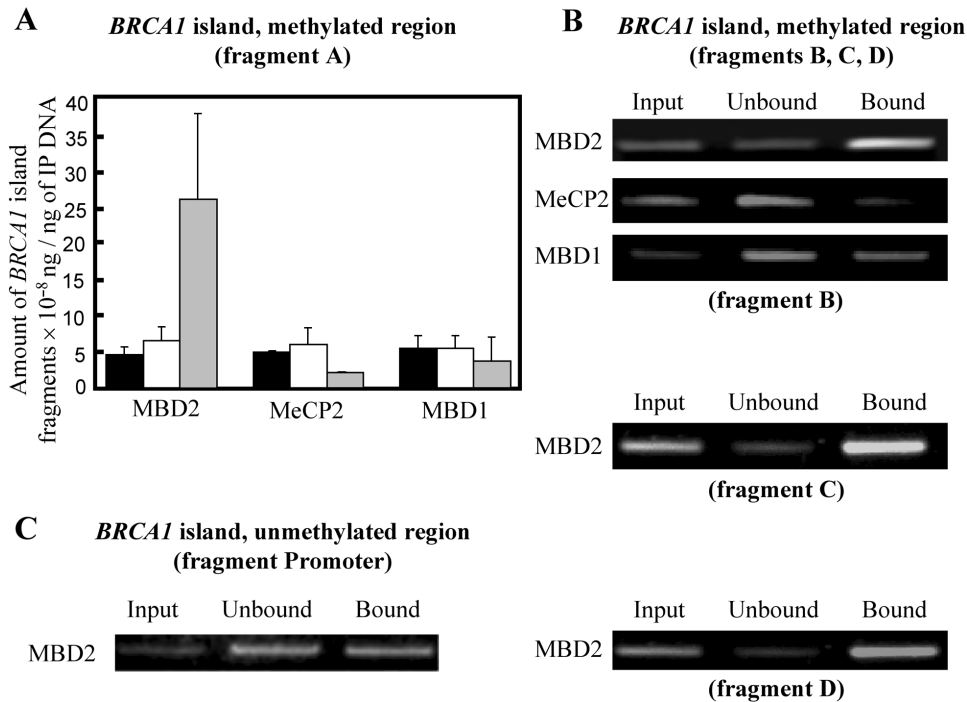


Figure 2. MBD2 associates the methylated region of the *BRCA1* CpG island in HeLa cells. (A) Amounts of immunoprecipitated *BRCA1* island (fragment A, see Figure 1) measured by competitive PCR (error bars, SD from, at least, three independent experiments). Cross-linked chromatin was immunoprecipitated using rabbit polyclonal anti-MBD2, anti-MeCP2, anti-MBD1 or monoclonal mouse anti-MBD1 antibodies. Purified DNA from the input, unbound or bound fractions was quantified and quantitative PCR analysis was accomplished. Then, the intensity of the bands corresponding to the PCR products was plotted against the initial number of competitor molecules as described in Supplementary Data, Figure 8s. Black box, amount of *BRCA1* island fragments per ng of the input DNA. Open box, amount of *BRCA1* island fragments per ng of the unbound DNA. Gray box, amount of *BRCA1* island fragments per ng of the bound DNA. (B) Three other regions of the *BRCA1* CpG island were analyzed by ChIP. These regions, fragments B, C and D (Figure 1), are located upstream the first region amplified by competitive PCR. After immunoprecipitation, purified DNA from the different fractions was quantified and 0.5 ng of this DNA was amplified. The intensities of the bands corresponding to the PCR products amplified from the input, unbound and bound fractions are shown. (C) Representative experiment of PCR amplification of an unmethylated region including the promoter and the exon 1 of the *BRCA1* gene ('promoter fragment' from position -56 to +263 bp from the *BRCA1* transcription start site) on MBD2-ChIP fractions.

DNA segment is less abundant in the bound fraction than in the input and the unbound fractions (Figure 2A).

A dose-dependent amplification of the 'B' region (nt -1364 to -1218) was performed on each fraction obtained from the ChIP procedure (Figure 2B). As observed at the segment lying

from position -1244 to -1004, enrichment in *BRCA1-NBR2* CpG island DNA in the bound fraction is only observed when the chromatin is immunoprecipitated with anti-MBD2 antibodies, while ChIPs with anti-MeCP2 or anti-MBD1 antibodies lead to a depletion of this DNA in the bound

fractions (Figure 2B). MBD2 binding to the methylated part of the repeated LTR12c element was further investigated by performing ChIP assays at the 'C' region (nt -1389 to -1637) and 'D' region (nt -1653 to -1928). A significant enrichment of these fragments in the chromatin fraction immunoprecipitated by antibodies against MBD2 was observed (Figure 2B).

We also amplified an unmethylated region containing the promoter and the exon 1 of the *BRCA1* gene (from position -56 to +263 bp from the *BRCA1* transcription start site). As expected, enrichment in *BRCA1-NBR2* CpG island was not observed in the chromatin fraction immunoprecipitated with anti-MBD2 antibodies (Figure 2C), since the amplified segment is unmethylated in HeLa cells (28). Taken together, these data strongly suggest that the methylated region of the *BRCA1-NBR2* CpG island is only bound by MBD2 in HeLa cells and that MBD2 binds only to the methylated region.

Depletion of MBD2 is not compensated by the binding of MeCP2 or MBD1 at the methylated region of *BRCA1-NBR2* CpG island

HeLa cells contain ~20 times more *MBD2* than *MeCP2* transcripts (30). In addition, it has been shown that some methylated DNA regions are bound by multiple MBD proteins (15). Taken together, these data suggest that the specific binding of MBD2 to the *BRCA1-NBR2* CpG island might be a consequence of the relative concentrations of the MBD proteins in HeLa cells. To address this issue, MBD proteins binding patterns at this CpG island were investigated in HeLa cells depleted in MBD2. Stable clones, expressing a siRNA targeted to *MBD2* transcripts (*MBD2a* and *b* isoforms), were constructed by stable transfection of pSUPER vector (33) containing a *MBD2* specific insert.

In several HeLa clones, quantitative competitive RT-PCR assays indicated a constitutive reduction of 89–96% in *MBD2* mRNA level (Figure 3A, *MBD2* KD clones). Western blot analysis also showed a dramatic decrease in MBD2 proteins in these *MBD2* KD clones carrying the pSuper-*MBD2* transgene (Figure 3B). In addition, persistent suppression of *MBD2* expression is conserved after many passages since efficient *MBD2* knockdown is still observed after 2 months of continuous culture. Furthermore, the expression of *MeCP2* and *MBD1* was not affected in *MBD2* knockdown clones (KD clones) when compared with the wild-type HeLa cells (data not shown).

Quantitative ChIP assays from HeLa cells depleted in MBD2 proteins showed no *BRCA1-NBR2* CpG island enrichment in the bound fraction when chromatin is immunoprecipitated with anti-MBD2 antibodies (Figure 4A). Furthermore, as previously observed in HeLa cells, the immunoprecipitated fractions are depleted in the methylated island when anti-MeCP2 or anti-MBD1 were used (Figure 4A). The same results were obtained when a different antibody, anti-MBD1, was used (data not shown). In addition, a positive immunoprecipitation of MeCP2-bound chromatin has been obtained in another set of experiments (Figure 7A and B), and in KD cells additional ChIP control experiments indicated that MBD1 proteins were associated with juxtacentromeric sequences *Sat2* (data not shown). Thus, in MBD2-depleted HeLa cells, the methylated region (nt -1244 to -1004) of

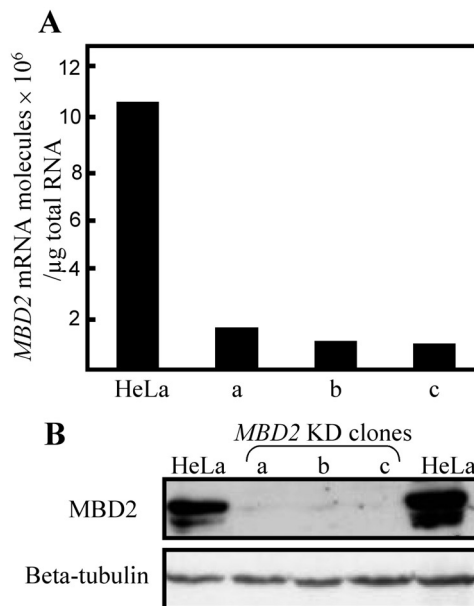


Figure 3. *MBD2* mRNA and protein quantification in HeLa cells expressing stable siRNA (*MBD2* knockdown cells). (A) Quantification of *MBD2* mRNA by competitive RT-PCR assay in wild-type HeLa and three clones of *MBD2* knockdown cells (a, b and c) performed from 0.1 μg of total RNA mixed with increasing amount of competitor *MBD2* RNA. The intensity of the bands corresponding to the PCR products was plotted against the initial number of competitor molecules in order to estimate the amount of *MBD2* mRNA present in 1 μg of each sample. (B) Immunoblot analysis of MBD2 proteins in HeLa and knockdown cell lines. MBD2 proteins were probed using a rabbit polyclonal antibody. Then, the same membrane was probed using a mouse β-tubulin antibody as a loading control.

BRCA1-NBR2 CpG island is not bound by these other two MBD proteins. This observation was extended to the adjacent methylated sequences (nt -1364 to -1218) using a semi-quantitative approach (Figure 4B). Taken together, these data indicate that the methylated region of the *BRCA1* island remains free from MeCP2 or MBD1 in MBD2-depleted HeLa cells, suggesting that MBD2 binding is specific.

Transcriptional repression of the *BRCA1-NBR2* locus by MBD2

The bidirectional promoter, driving both *BRCA1* and *NBR2* expression, is relatively far (~1 kb) from the methylated domain of the CpG island. However, in human cell lines, chemically induced demethylation stimulates *BRCA1* gene expression and *in vitro* methylated expression vectors carrying this CpG island is repressed when transiently transfected into human cell lines (28). Since *NBR2* and *BRCA1* share the same promoter region (Figure 1), we tested a potential role of DNA methylation in the expression of the *NBR2* gene. In HeLa cells, demethylation was induced by 5-aza-dC treatments. *NBR2* transcripts were then quantified using a competitive RT-PCR method (a representative assay is shown in Figure 5A). As described previously (28), 5-aza-dC treatment of HeLa cells elevated *BRCA1* expression by 1.8-fold and an overexpression of *NBR2* (3.1-fold) was also observed (Figure 5B).

These data raised the question whether MBD2 is a methylation-dependent repressor of the *BRCA1-NBR2*

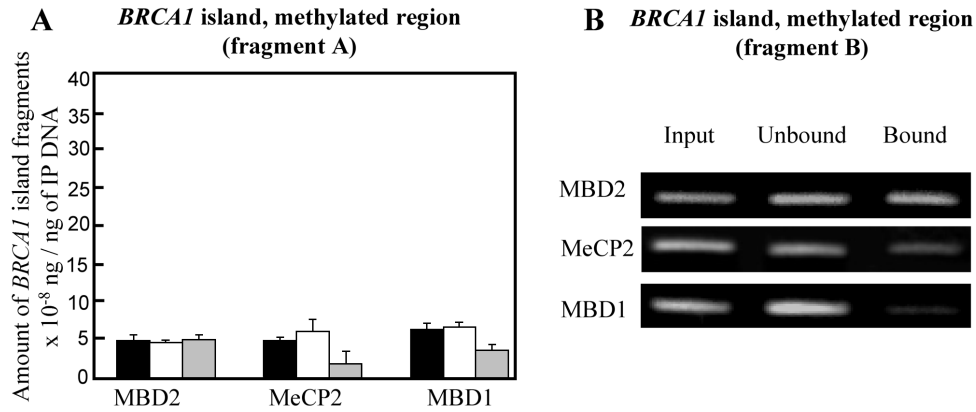


Figure 4. MeCP2 and MBD1 do not compensate for MBD2 depletion at the *BRCA1-NBR2* CpG island in *MBD2* knockdown HeLa cells. (A) Amounts of immunoprecipitated *BRCA1* island (fragment A, Figure 1) measured by competitive PCR (error bars, SD from, at least, three independent experiments). Black box, amount of *BRCA1* island fragments per ng of the input DNA. Open box, amount of *BRCA1* island fragments per ng of the unbound DNA. Gray box, amount of *BRCA1* island fragments per ng of the bound DNA. (B) Representative examples of *BRCA1* semi-quantitative PCR (fragment B, Figure 1) on MBDs-ChIP assays (as described in Figure 2B).

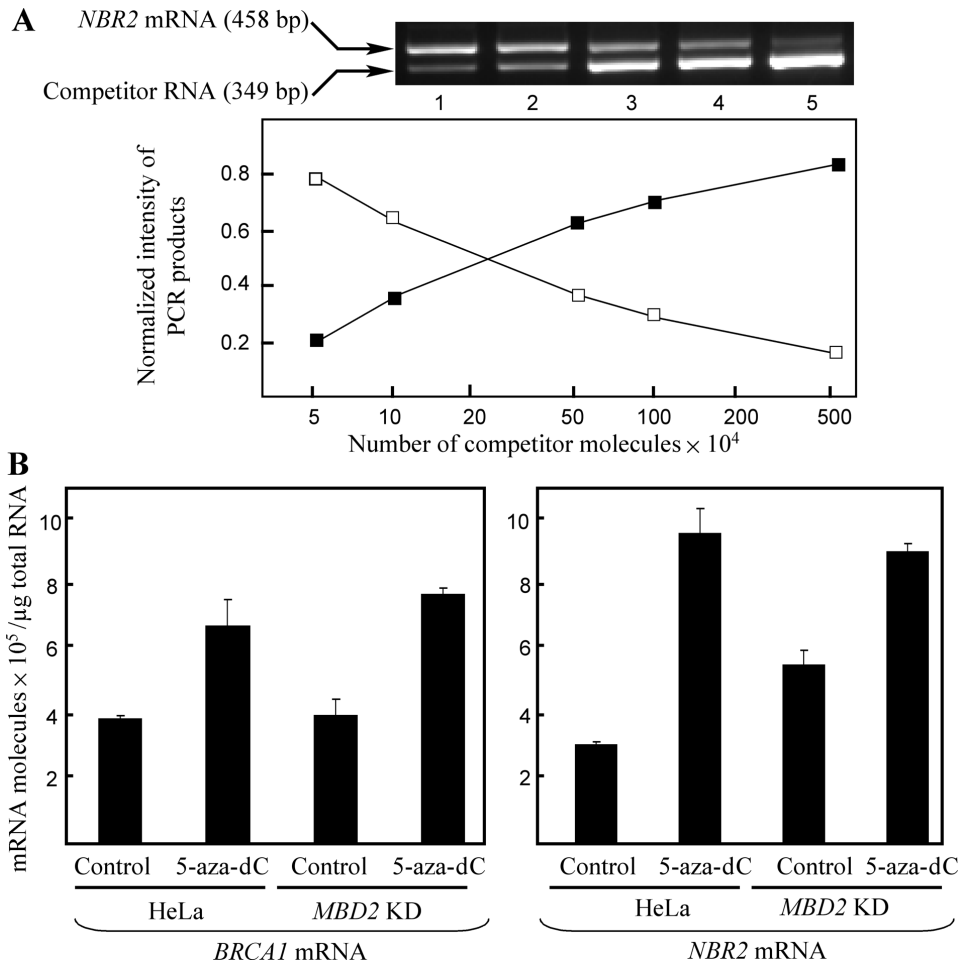


Figure 5. Effects of 5-aza-dC on the expression of *BRCA1* and *NBR2* in HeLa and *MBD2* knockdown cells. (A) Quantitative competitive RT-PCR assay of *NBR2* mRNAs was performed from 0.6 μg of total RNA mixed with increasing amount of *NBR2* competitor RNA. Amounts of competitor molecules: lane 1, 5×10^4 ; lane 2, 10^5 ; lane 3, 5×10^5 ; lane 4, 10^6 ; lane 5, 5×10^6 . The RT-PCR products were analyzed on a 2% agarose gel containing ethidium bromide. The intensity of the bands corresponding to the PCR products was plotted against the initial number of competitor molecules. The diagrams of the intensity values are represented below the gels. Black box, 349 bp band competitor *NBR2* RNA; open box, 458 bp band endogenous *NBR2* RNA. (B) *NBR2* and *BRCA1* transcripts in HeLa cells and *MBD2* KD cells treated or untreated with 10 μM 5-aza-dC for 72 h. Quantitative RT-PCR analyses were performed from 0.6 μg of total RNA mixed with increasing amount of competitor *NBR2* RNA or from 0.3 μg of total RNA mixed with increasing amount of competitor *BRCA1* RNA (32). Average values obtained from four independent experiments (error bar, SD) are shown. Control: untreated cells.

bidirectional promoter. In MBD2 depleted cells, a stimulation of *NBR2* expression by 1.7-fold is observed when compared with wild-type HeLa cells (Figure 5B). In addition, in *MBD2* KD clones, 5-aza-dC treatments (Figure 5B) had a lower effect (1.6-fold) on *NBR2* expression than in wild-type cells (3.1-fold). Since both cell types exhibit the same amount of *NBR2* transcripts after 5-aza-dC treatments (Figure 5B), these data suggest that MBD2 is an important factor in the *NBR2* methylation-dependent control.

However, the same amounts of *BRCA1* transcripts were found in *MBD2* KD clones and in wild-type HeLa cells (Figure 5B). In addition, *BRCA1* response to 5-aza-dC treatment is not modified by MBD2 depletion (Figure 5B), indicating that *BRCA1* expression is independent of the MBD2 binding. Furthermore, control experiments indicated that the methylation pattern of *BRCA1-NBR2* CpG island was not modified in *MBD2* KD cells when compared with the wild-type HeLa cells (Supplementary Data, Figure 9s). Taken together, these data suggest a specific methylation-dependent repression of *NBR2* by MBD2.

Mbd2 expression rescues the reduction of *NBR2* transcript in *MBD2* knockdown clones

Functional control of the specific repression of *NBR2* by MBD2 has been performed by expressing the *MBD2* target-cDNA in a form that is refractory to siRNA-mediated decay. Five silent point mutations of the third-codon within the targeted region were introduced into a mouse *Mbd2* cDNA and the resulting expression vector (pRev-MBD2) was transiently expressed in *MBD2* KD clones after transfection. Western blot analysis of HeLa and *MBD2* KD clones indicated that Mbd2 proteins were efficiently expressed from the pRev-MBD2 expression vector (Figure 6A).

In wild-type HeLa cells, the level of *BRCA1* and *NBR2* transcripts was not affected by the Mbd2 overexpression due to the pRev-MBD2 vector (Figure 6B). Also, the pCMV-MBD2 expression vector containing a non-mutated mouse *Mbd2* cDNA did not alter *BRCA1* and *NBR2* transcription in HeLa cells (data not shown). Therefore, the amount of MBD2 is not a limiting factor in the transcriptional repression of the *BRCA1-NBR2* locus, in HeLa cells. In contrast, in *MBD2* KD cells, pRev-MBD2 expression induced a 28–45% decrease in *NBR2* expression (Figure 6B) and transfected *MBD2* KD cells exhibited an *NBR2* mRNA level equivalent to the level observed in wild-type HeLa cells. No statistically significant decrease in *BRCA1* mRNA level was observed in these transfected *MBD2* KD cells (Figure 6B). These data confirm that, at the *BRCA1-NBR2* locus, MBD2 specifically represses the *NBR2* gene.

Specificity of transcriptional repression by MBD2

Taken together, these data indicate that, in HeLa cells, under physiological concentrations, MBD2 binds to the *BRCA1-NBR2* CpG island and the absence of this protein is not compensated by the binding of other MBD proteins. However, experiments have suggested that exogenous *BRCA1* might be repressed by the overexpression of MeCP2 (28). We have, therefore, investigated the ability of the exogenous MeCP2 to repress the transcription of the endogenous locus. *Mecp2* was overexpressed in HeLa and *MBD2* KD cells by

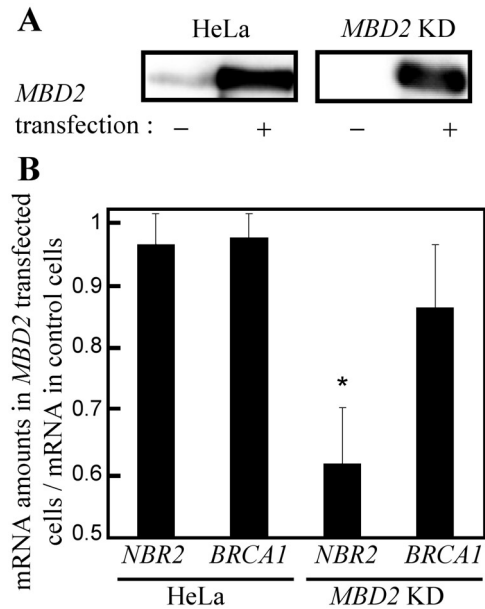


Figure 6. MBD2 transfection experiments in HeLa and *MBD2* knockdown cells. (A) Immunoblot analysis of MBD2 proteins in HeLa and *MBD2* KD cells transfected with an MBD2 vector expressing a transcript resistant to RNAi (pRev-MBD2 vector). HeLa and *MBD2* KD cells were transfected with the pRev-MBD2 vector or with an empty pGL3 basic vector (pGL3). MBD2 proteins, from whole cell extract prepared 48 h after transfection, were probed using a rabbit polyclonal antibody. (B) Quantitative RT-PCR analysis of *BRCA1* and *NBR2* transcripts was performed (as described in Figure 5) from HeLa and *MBD2* KD cells transfected with the pRev-MBD2 or an empty vector (pGL3). The ratio between the amounts of the transcripts in pRev-MBD2-transfected cells and pGL3-transfected cells was then calculated. Mean values obtained from at least four independent transfection experiments are shown [**P* = 0.0049 (<0.05), *t*-test].

transient transfection of the pCMV-MeCP2-Ha vector. Immunoblots indicated a high expression of MeCP2 after transfection in both cell types (Supplementary Data, Figure 10s).

Quantitative ChIP assays, from transfected *MBD2* KD cells, showed a slight (~1.7-fold) but statistically significant enrichment in the A segment of *BRCA1-NBR2* CpG island (Figure 1, 'A' segment) in the chromatin fraction immunoprecipitated by antibodies against MeCP2 (Figure 7A). MeCP2 binding was further confirmed by a semi-quantitative ChIP in the adjacent region (Figure 7B). This MeCP2 binding is associated with a decrease (17–26%) in *NBR2* transcripts (Figure 7C), when compared to *MBD2* KD cells transfected with an empty vector. In addition, in HeLa cells, overexpression of MeCP2 did not modify *NBR2* transcription, as observed after pRev-MBD2 transfections (Figure 7C). *BRCA1* mRNA amounts remain unchanged in both wild-type and *MBD2* KD HeLa cells expressing MeCP2 at a high level (Figure 7C). Thus, in *MBD2* depleted cells, elevated level of exogenous MeCP2 leads to MeCP2 binding at the *BRCA1-NBR2* locus and to a partial repression of *NBR2*.

DISCUSSION

Transient transfection of *in vitro* methylated expression vectors has clearly demonstrated that members of the methyl-CpG binding protein family, MBD1, MBD2 and MeCP2, are directly involved in the methylation-dependent repression of

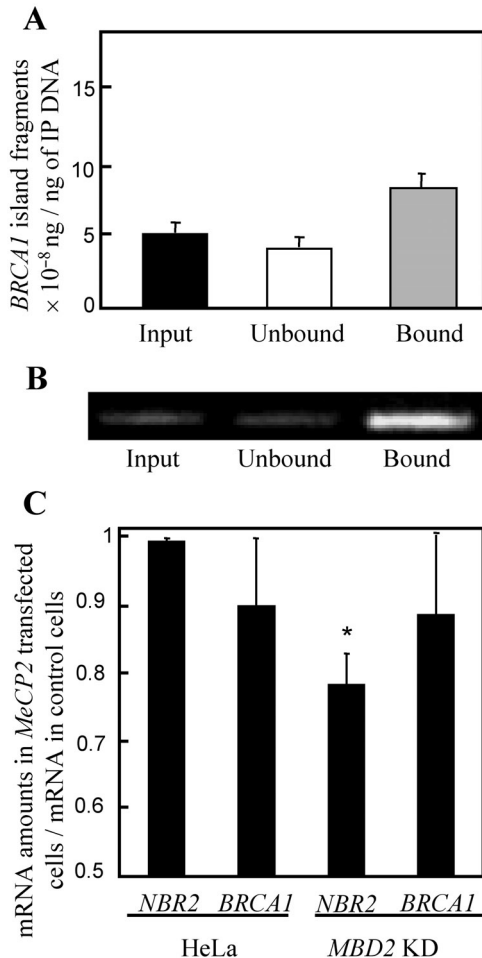


Figure 7. MeCP2 transfection experiments in HeLa and *MBD2* knockdown cells. (A) Quantitative MeCP2-ChIP assays in *MBD2* KD cells transfected with the pCMV-MeCP2-HA vector. After immunoprecipitation of cross-linked chromatin with an anti-MeCP2 antibody, competitive PCR analysis (fragment A, Figure 1) was performed (as described in Figure 2). Average values obtained from two independent MeCP2-ChIP assays are shown. (B) A representative example of a *BRCA1* semi-quantitative PCR (fragment B, Figure 1) performed on these ChIP assays. See Supplementary Results for immunoblot controls (Supplementary Figure 10s). (C) *BRCA1* and *NBR2* mRNA quantification in HeLa and *MBD2* KD cells transfected with an MeCP2 vector. Four independent transfection experiments of HeLa and *MBD2* KD cells with the pCMV-MeCP2-HA vector or an empty pGL3 basic vector (pGL3), RNA extraction and quantitative RT-PCR analysis were performed. Average values are presented on this graph [$*P = 0.018$ (< 0.05), *t*-test].

gene expression (1). In the mouse, loss of these proteins leads to a prominent effect on cerebral function (17–19), suggesting a specific dependence of these tissues on the control mediated by MBD proteins. Alternatively, functional redundancy between MBD proteins may be more important in other tissues. In line with this hypothesis, global gene overexpression was not observed in mice lacking a particular MBD protein (17–20). Nevertheless, further studies indicated that gene-specific dysregulation in non-cerebral tissues are associated with the loss of MBD proteins (21,22,24). Analysis of the chromatin proteins also raises the question of the redundancy between these proteins.

Our analysis, in the HeLa cell line, of a CpG island at the *BRCA1-NBR2* locus indicates that the methylated part of this

CpG island is bound by MBD2 while MeCP2 and MBD1 are not detected in this region. Furthermore, western blot analysis, using antibodies directed against MeCP2 and MBD1 produced a signal at the expected size (15), ~85 and ~70 kDa, respectively, indicating that both proteins are expressed in this cell line (data not shown). Thus, the lack of detection of these two proteins at the methylated region of the *BRCA1-NBR2* CpG island is not due to their absence. In addition, the depletion in *BRCA1-NBR2* CpG island in the chromatin fractions immunoprecipitated by the anti-MeCP2 and MBD1 antibodies also indicates that these two proteins are linked to other chromatin domains in HeLa cells. Therefore, the methylated part of this CpG island seems to be specifically associated with MBD2 in our cellular model. Although all the MBD proteins are ubiquitously expressed in somatic tissues, variations in their expression levels, depending on the cell type and the differentiation state, have been observed previously (35). For example, in mouse brain, *Mecp2* and *Mbd1* are highly expressed when compared with *Mbd2* (2), while *MBD2* transcripts are 20-fold more abundant than *Mecp2* mRNA in breast tissues (30), suggesting that the relative MBD protein concentrations might be involved in the phenotypes associated with their experimental depletions. Therefore, their relative concentrations might be associated with a prominent binding of MBD2 to some methylated DNA segments. However, in these cells, the strong targeted-depletion of MBD2 proteins, induced by RNAi, does not induce the binding of other MBD proteins at the methylated region of the *BRCA1-NBR2* CpG island. Thus, these data suggest that this sequence is a preferential target for MBD2.

Among the mechanisms potentially involved in the preferential binding of MBD2, differences in affinity for methylated DNA might be an important component, since it was shown that murine *Mbd2b* exhibits a higher affinity than *Mecp2* for methylated oligonucleotides (36). Although this possibility cannot be excluded, it should be noted that, in *MBD2* knockdown HeLa clones, *MBD2* proteins were nearly undetectable and the amount of the transcripts was reduced by 92% on the average, while MeCP2 and MBD1 protein levels remained unchanged (data not shown). In addition, hypermethylated CpG islands are associated with MeCP2 in several cell lines and tissues expressing all MBD proteins (14,15,37,38) and when overexpressed in HeLa cells depleted in MBD2 proteins, *Mecp2* binds to the *BRCA1-NBR2* CpG island. Taken together, these data suggest that corepressors of transcription leading to a non-permissive chromatin environment may be, *in vivo*, of importance for the specific recruitment of MBD2, or alternatively for the exclusion of MeCP2 and MBD1 at the *BRCA1-NBR2* locus. The possible presence of a recently described MBD2 partner, the MIZF protein (39), has also been investigated, since the methylated region of the *BRCA1-NBR2* CpG island contains a consensus binding site for this protein at position -960 bp. However, we failed to detect MIZF at this locus by ChIP (data not shown).

In human cell lines, while chemically induced hypomethylation was associated with the activation of both *BRCA1* and *NBR2*, transcriptional repression mediated by MBD2 seemed to be gene specific, since *MBD2* knockdown elevated only *NBR2* transcription, in HeLa cells. In addition, this phenotype was rescued by exogenous *Mbd2*, indicating that this effect is a specific consequence of the *MBD2* knockdown. Furthermore,

this latter experiment also confirmed that MBD2 is not involved in *BRCA1* expression, since the expression of exogenous *Mbd2* did not modify the amounts of *BRCA1* transcripts in both wild-type HeLa cells and *MBD2* KD cells. Moreover, the response of *NBR2* to DNA hypomethylation was reduced by a factor of ~ 2 in MBD2-depleted HeLa cells, while *BRCA1* response was not affected by the *MBD2*-siRNA. Although MBD2 depletion does not completely abolish the effect of 5-aza-dC, the consistent reduction of 5-aza-dC-response in MBD2-depleted HeLa cells confirms that MBD2 significantly contributes to the methylation-dependent *NBR2* repression.

In the human genome, *BRCA1* lies head to head with the *NBR2* gene (40). The transcription start site of *BRCA1* is separated from the *NBR2* gene by a 218 bp bidirectional promoter (40,41). This region is embedded within a large CpG island (13) and the methylated part of this region corresponds to a nuclease resistant chromatin structure in human breast cell lines (29) and in HeLa cells. Hence, this region is located at the 3' end of the *NBR2* transcription start site and at the 5' end of *BRCA1* (Figure 1). The specificity of MBD2 towards *NBR2* transcription from the bidirectional *BRCA1-NBR2* promoter, suggests that the methylation-dependent repression of *NBR2* and *BRCA1* is mediated by different mechanisms.

The analysis of the 5' region of the endothelin receptor B gene in human cell lines shows that extensive methylation closely downstream of the initiation site does not abolish gene expression (42). However, studies using plasmid and episomal vectors (43–45) and patch methylation techniques indicate that methylation downstream of a promoter can decrease transcription levels, suggesting that this epigenetic mark may also affect the elongation rate. Therefore, the reduced expression of *NBR2* mediated by MBD2 might be dependent on such mechanisms. In line with this hypothesis, *BRCA1* expression is not affected by MBD2 binding to the methylated region of the CpG island upstream its promoter. Nevertheless, inhibition of DNA methylation stimulates *BRCA1* expression, suggesting that its repression might be associated with the binding of different MBD proteins to some other methylated DNA segments. Alternatively, DNA methylation may have a direct effect on the binding of regulatory factors since it was suggested that the -1582 to -202 region of the 5' end of *BRCA1* contains several weak regulatory sites (both enhancers and repressors) with additive effects (40) and a putative cAMP-responsive element binding transcription factor binding site has been mapped in the *BRCA1* promoter (46).

MBD2 belongs to a family of methylation-dependent transcriptional repressor and its presence in aberrantly methylated genes has been observed in human cancer cell lines (47–49). However, a direct relationship between MBD2 binding and gene repression has been established only for a few genes. In mouse, it had been shown that Gata-3 and Mbd2 act in competition for the regulation of *I14* gene transcription in T-helper cells (49). Evidences for a contribution of MBD2 in silencing the aberrantly methylated pi-class glutathione S-transferase (*GSTP1*) promoter have been obtained, in the breast cancer cell line MCF7 cells, by MBD2-depletion mediated by siRNA (48).

Functional domains have been mapped within the MBD proteins and beside their methyl-CpG binding domain, all these proteins possess a domain involved in gene repression,

the transcriptional repression domains (TRDs); in contrast to the MBD, no sequence similarities were found between the different TRDs (1). Many promoters, including Simian virus 40, cytomegalovirus and beta-actin promoters (3), are efficiently repressed by tethering the minimal TRD of MeCP2, MBD1 and MBD2. However, it was shown that the *L1* promoter is not repressed by fusion protein containing the TRD of MBD2, but is silenced by fusion proteins containing either MeCP2 or MBD1 TRDs (50). The repression of *NBR2* by MBD2 does not seem to be specific of its TRD, since in MBD2-depleted HeLa cells, exogenous *Mecp2* decreased *NBR2* transcription. Similarly, inhibitory effect of exogenous *Mecp2* has already been observed in *Mbd2*^{-/-} mice. Indeed, previous studies have shown that the methylation-dependent repression of reporter genes is impaired in fibroblast cell lines from these mice, suggesting that endogenous *Mecp2* proteins do not compensate for the absence of Mbd2 (18). Nevertheless, exogenous *Mecp2* restores full repression in the *Mbd2*^{-/-} cells, indicating that the overexpression of *Mecp2* can counteract the absence of *Mbd2* in this system (18).

Although *Mbd2*^{-/-} mice are viable and fertile (20), a reduction in Mbd2 inhibits the development of intestinal adenomas in the tumor-prone *Apc*^{Min/+} mouse (51). In human cell lines, *MBD2* antisense inhibitors suppress tumorigenesis *in vitro* and *in vivo*, when these cells are implanted in nude mice as a model (52). Taken together these data suggest that MBD2 represents a new target potential in cancer therapy and, therefore, new insights on MBD2 specificities are, in this context, of importance. Collectively, our data indicate that MBD2 specifically binds to the *BRCA1* island and represses *NBR2*. In addition, our results suggest that the relative abundance of MBD is not a major factor in their targeting to some methylated DNAs. Furthermore, the cellular model developed in this study may represent a valuable tool for the identification of MBD2 target genes, which could be valuable for therapeutics applications.

SUPPLEMENTARY MATERIAL

Supplementary Material is available at NAR Online.

ACKNOWLEDGEMENTS

We are most grateful to Dr Paul Wade for providing MBD2 antibodies and to Dr Adrian Bird for the pCMV-MeCP2-HA and pCMV-MBD2 vectors. This work was supported by the Ligue Nationale contre le Cancer (Comité du Rhône and Comité de la Loire), France and the Association pour la Recherche sur le Cancer, France. Funding to pay the Open Access publication charges for this article was provided by Centre Leon Berard, Lyon, France.

Conflict of interest statement. None declared.

REFERENCES

- Bird, A.P. and Wolffe, A.P. (1999) Methylation-induced repression—belts, braces, and chromatin. *Cell*, **99**, 451–454.
- Hendrich, B. and Bird, A. (1998) Identification and characterization of a family of mammalian methyl-CpG binding proteins. *Mol. Cell. Biol.*, **18**, 6538–6547.

3. Wade, P.A. (2001) Methyl CpG-binding proteins and transcriptional repression. *Bioessays*, **23**, 1131–1137.
4. Fuks, F., Hurd, P.J., Wolf, D., Nan, X., Bird, A.P. and Kouzarides, T. (2003) The methyl-CpG-binding protein MeCP2 links DNA methylation to histone methylation. *J. Biol. Chem.*, **278**, 4035–4040.
5. Jones, P.L., Veenstra, G.J., Wade, P.A., Vermaak, D., Kass, S.U., Landsberger, N., Strouboulis, J. and Wolffe, A.P. (1998) Methylated DNA and MeCP2 recruit histone deacetylase to repress transcription. *Nature Genet.*, **19**, 187–191.
6. Nan, X., Ng, H.H., Johnson, C.A., Laherty, C.D., Turner, B.M., Eisenman, R.N. and Bird, A. (1998) Transcriptional repression by the methyl-CpG-binding protein MeCP2 involves a histone deacetylase complex. *Nature*, **393**, 386–389.
7. Ng, H.H., Zhang, Y., Hendrich, B., Johnson, C.A., Turner, B.M., Erdjument-Bromage, H., Tempst, P., Reinberg, D. and Bird, A. (1999) MBD2 is a transcriptional repressor belonging to the MeCP1 histone deacetylase complex. *Nature Genet.*, **23**, 58–61.
8. Wade, P.A., Geggion, A., Jones, P.L., Ballestar, E., Aubry, F. and Wolffe, A.P. (1999) Mi-2 complex couples DNA methylation to chromatin remodelling and histone deacetylation. *Nature Genet.*, **23**, 62–66.
9. Boeke, J., Ammerpohl, O., Kegel, S., Moehren, U. and Renkawitz, R. (2000) The minimal repression domain of MBD2b overlaps with the methyl-CpG-binding domain and binds directly to Sin3A. *J. Biol. Chem.*, **275**, 34963–34967.
10. Ng, H.H., Jeppesen, P. and Bird, A. (2000) Active repression of methylated genes by the chromosomal protein MBD1. *Mol. Cell. Biol.*, **20**, 1394–1406.
11. Fujita, N., Watanabe, S., Ichimura, T., Tsuruzoe, S., Shinkai, Y., Tachibana, M., Chiba, T. and Nakao, M. (2003) Methyl-CpG binding domain 1 (MBD1) interacts with the Suv39h1-HP1 heterochromatic complex for DNA methylation-based transcriptional repression. *J. Biol. Chem.*, **278**, 24132–24138.
12. Sarraf, S.A. and Stancheva, I. (2004) Methyl-CpG binding protein MBD1 couples histone H3 methylation at lysine 9 by SETDB1 to DNA replication and chromatin assembly. *Mol. Cell*, **15**, 595–605.
13. Smith, T.M., Lee, M.K., Szabo, C.I., Jerome, N., McEuen, M., Taylor, M., Hood, L. and King, M.C. (1996) Complete genomic sequence and analysis of 117 kb of human DNA containing the gene BRCA1. *Genome Res.*, **6**, 1029–1049.
14. Fournier, C., Goto, Y., Ballestar, E., Delaval, K., Hever, A.M., Esteller, M. and Feil, R. (2002) Allele-specific histone lysine methylation marks regulatory regions at imprinted mouse genes. *EMBO J.*, **21**, 6560–6570.
15. Ballestar, E., Paz, M.F., Valle, L., Wei, S., Fraga, M.F., Espada, J., Cigudosa, J.C., Huang, T.H. and Esteller, M. (2003) Methyl-CpG binding proteins identify novel sites of epigenetic inactivation in human cancer. *EMBO J.*, **22**, 6335–6345.
16. Amir, R.E., Van den Veyver, I.B., Wan, M., Tran, C.Q., Francke, U. and Zoghbi, H.Y. (1999) Rett syndrome is caused by mutations in X-linked MECP2, encoding methyl-CpG-binding protein 2. *Nature Genet.*, **23**, 185–188.
17. Chen, R.Z., Akbarian, S., Tudor, M. and Jaenisch, R. (2001) Deficiency of methyl-CpG binding protein-2 in CNS neurons results in a Rett-like phenotype in mice. *Nature Genet.*, **27**, 327–331.
18. Guy, J., Hendrich, B., Holmes, M., Martin, J.E. and Bird, A. (2001) A mouse MeCP2-null mutation causes neurological symptoms that mimic Rett syndrome. *Nature Genet.*, **27**, 322–326.
19. Zhao, X., Ueba, T., Christie, B.R., Barkho, B., McConnell, M.J., Nakashima, K., Lein, E.S., Eadie, B.D., Willhoite, A.R., Muotri, A.R. et al. (2003) Mice lacking methyl-CpG binding protein 1 have deficits in adult neurogenesis and hippocampal function. *Proc. Natl Acad. Sci. USA*, **100**, 6777–6782.
20. Hendrich, B., Guy, J., Ramsahoye, B., Wilson, V.A. and Bird, A. (2001) Closely related proteins MBD2 and MBD3 play distinctive but interacting roles in mouse development. *Genes Dev.*, **15**, 710–723.
21. Chen, W.G., Chang, Q., Lin, Y., Meissner, A., West, A.E., Griffith, E.C., Jaenisch, R. and Greenberg, M.E. (2003) Derepression of BDNF transcription involves calcium-dependent phosphorylation of MeCP2. *Science*, **302**, 885–889.
22. Martinowich, K., Hattori, D., Wu, H., Fouse, S., He, F., Hu, Y., Fan, G. and Sun, Y.E. (2003) DNA methylation-related chromatin remodeling in activity-dependent BDNF gene regulation. *Science*, **302**, 890–893.
23. Horike, S., Cai, S., Miyano, M., Cheng, J.F. and Kohwi-Shigematsu, T. (2005) Loss of silent-chromatin looping and impaired imprinting of DLX5 in Rett syndrome. *Nature Genet.*, **37**, 31–40.
24. Hutchins, A.S., Mullen, A.C., Lee, H.W., Sykes, K.J., High, F.A., Hendrich, B.D., Bird, A.P. and Reiner, S.L. (2002) Gene silencing quantitatively controls the function of a developmental *trans*-activator. *Mol. Cell*, **10**, 81–91.
25. Koch, C. and Stratling, W.H. (2004) DNA binding of methyl-CpG-binding protein MeCP2 in human MCF7 cells. *Biochemistry*, **43**, 5011–5021.
26. Xu, C.F., Brown, M.A., Nicolai, H., Chambers, J.A., Griffiths, B.L. and Solomon, E. (1997) Isolation and characterisation of the *NBR2* gene which lies head to head with the human *BRCA1* gene. *Hum. Mol. Genet.*, **6**, 1057–1062.
27. Butcher, D.T., Mancini-DiNardo, D.N., Archer, T.K. and Rodenhiser, D.I. (2004) DNA binding sites for putative methylation boundaries in the unmethylated region of the *BRCA1* promoter. *Int. J. Cancer*, **111**, 669–678.
28. Magdinier, F., Billard, L.M., Wittmann, G., Frappart, L., Benchaib, M., Lenoir, G.M., Guerin, J.F. and Dante, R. (2000) Regional methylation of the 5' end CpG island of *BRCA1* is associated with reduced gene expression in human somatic cells. *FASEB J.*, **14**, 1585–1594.
29. Rice, J.C. and Futscher, B.W. (2000) Transcriptional repression of *BRCA1* by aberrant cytosine methylation, histone hypoacetylation and chromatin condensation of the *BRCA1* promoter. *Nucleic Acids Res.*, **28**, 3233–3239.
30. Billard, L.M., Magdinier, F., Lenoir, G.M., Frappart, L. and Dante, R. (2002) MeCP2 and MBD2 expression during normal and pathological growth of the human mammary gland. *Oncogene*, **21**, 2704–2712.
31. Magdinier, F., Dalla Venezia, N., Lenoir, G.M., Frappart, L. and Dante, R. (1999) *BRCA1* expression during prenatal development of the human mammary gland. *Oncogene*, **18**, 4039–4043.
32. Ribieras, S., Magdinier, F., Leclerc, D., Lenoir, G., Frappart, L. and Dante, R. (1997) Abundance of *BRCA1* transcripts in human cancer and lymphoblastoid cell lines carrying *BRCA1* germ-line alterations. *Int. J. Cancer*, **73**, 715–718.
33. Brummelkamp, T.R., Bernards, R. and Agami, R. (2002) A system for stable expression of short interfering RNAs in mammalian cells. *Science*, **296**, 550–553.
34. Frommer, M., McDonald, L.E., Millar, D.S., Collis, C.M., Watt, F., Grigg, G.W., Molloy, P.L. and Paul, C.L. (1992) A genomic sequencing protocol that yields a positive display of 5-methylcytosine residues in individual DNA strands. *Proc. Natl Acad. Sci. USA*, **89**, 1827–1831.
35. Meehan, R.R., Lewis, J.D. and Bird, A.P. (1992) Characterization of MeCP2, a vertebrate DNA binding protein with affinity for methylated DNA. *Nucleic Acids Res.*, **20**, 5085–5092.
36. Fraga, M.F., Ballestar, E., Montoya, G., Taysavang, P., Wade, P.A. and Esteller, M. (2003) The affinity of different MBD proteins for a specific methylated locus depends on their intrinsic binding properties. *Nucleic Acids Res.*, **31**, 1765–1774.
37. El-Osta, A., Kantharidis, P., Zalberg, J.R. and Wolffe, A.P. (2002) Precipitous release of methyl-CpG binding protein 2 and histone deacetylase 1 from the methylated human multidrug resistance gene (*MDR1*) on activation. *Mol. Cell. Biol.*, **22**, 1844–1857.
38. Nguyen, C.T., Gonzales, F.A. and Jones, P.A. (2001) Altered chromatin structure associated with methylation-induced gene silencing in cancer cells: correlation of accessibility, methylation, MeCP2 binding and acetylation. *Nucleic Acids Res.*, **29**, 4598–4606.
39. Sekimata, M. and Homma, Y. (2004) Sequence-specific transcriptional repression by an MBD2-interacting zinc finger protein MIZF. *Nucleic Acids Res.*, **32**, 590–597.
40. Thakur, S. and Croce, C.M. (1999) Positive regulation of the *BRCA1* promoter. *J. Biol. Chem.*, **274**, 8837–8843.
41. Xu, C.F., Chambers, J.A. and Solomon, E. (1997) Complex regulation of the *BRCA1* gene. *J. Biol. Chem.*, **272**, 20994–20997.
42. Pao, M.M., Tsutsumi, M., Liang, G., Uzvolgyi, E., Gonzales, F.A. and Jones, P.A. (2001) The endothelin receptor B (*EDNRB*) promoter displays heterogeneous, site specific methylation patterns in normal and tumor cells. *Hum. Mol. Genet.*, **10**, 903–910.
43. Hsieh, C.L. (1997) Stability of patch methylation and its impact in regions of transcriptional initiation and elongation. *Mol. Cell. Biol.*, **17**, 5897–5904.
44. Kass, S.U., Goddard, J.P. and Adams, R.L. (1993) Inactive chromatin spreads from a focus of methylation. *Mol. Cell. Biol.*, **13**, 7372–7379.

45. Lorincz, M.C., Dickerson, D.R., Schmitt, M. and Groudine, M. (2004) Intragenic DNA methylation alters chromatin structure and elongation efficiency in mammalian cells. *Nature Struct. Mol. Biol.*, **11**, 1068–1075.
46. Mancini, D.N., Rodenhiser, D.I., Ainsworth, P.J., O'Malley, F.P., Singh, S.M., Xing, W. and Archer, T.K. (1998) CpG methylation within the 5' regulatory region of the *BRCA1* gene is tumor specific and includes a putative CREB binding site. *Oncogene*, **16**, 1161–1169.
47. Ballestar, E. and Wolffe, A.P. (2001) Methyl-CpG-binding proteins. Targeting specific gene repression. *Eur. J. Biochem.*, **268**, 1–6.
48. Lin, X. and Nelson, W.G. (2003) Methyl-CpG-binding domain protein-2 mediates transcriptional repression associated with hypermethylated GSTP1 CpG islands in MCF-7 breast cancer cells. *Cancer Res.*, **63**, 498–504.
49. Magdinier, F. and Wolffe, A.P. (2001) Selective association of the methyl-CpG binding protein MBD2 with the silent p14/p16 locus in human neoplasia. *Proc. Natl Acad. Sci. USA*, **98**, 4990–4995.
50. Yu, F., Zingler, N., Schumann, G. and Stratling, W.H. (2001) Methyl-CpG-binding protein 2 represses LINE-1 expression and retrotransposition but not Alu transcription. *Nucleic Acids Res.*, **29**, 4493–4501.
51. Sansom, O.J., Berger, J., Bishop, S.M., Hendrich, B., Bird, A. and Clarke, A.R. (2003) Deficiency of Mbd2 suppresses intestinal tumorigenesis. *Nature Genet.*, **34**, 145–147.
52. Campbell, P.M., Bovenzi, V. and Szyf, M. (2004) Methylated DNA-binding protein 2 antisense inhibitors suppress tumorigenesis of human cancer cell lines *in vitro* and *in vivo*. *Carcinogenesis*, **25**, 499–507.